

# Investigation of the Exclusive ${}^3\text{He}(e, e'pp)n$ Reaction

D.L. Groep<sup>1</sup>, M.F. van Batenburg<sup>1</sup>, Th.S. Bauer<sup>1,2</sup>, H.P. Blok<sup>1,3</sup>, D.J. Boersma<sup>1,2</sup>, E. Cisbani<sup>4</sup>, R. De Leo<sup>5</sup>, S. Frullani<sup>4</sup>, F. Garibaldi<sup>4</sup>, W. Glöckle<sup>6</sup>, J. Golak<sup>7</sup>, P. Heimberg<sup>1,3</sup>, W.H.A. Hesselink<sup>1,3</sup>, M. Iodice<sup>4</sup>, D.G. Ireland<sup>8</sup>, E. Jans<sup>1,\*</sup>, H. Kamada<sup>6</sup>, L. Lapikás<sup>1</sup>, G.J. Lolos<sup>9</sup>, R. Perrino<sup>10</sup>, A. Scott<sup>8</sup>, R. Starink<sup>1,3</sup>, M.F.M. Steenbakkers<sup>1,3</sup>, G.M. Urciuoli<sup>4</sup>, H. de Vries<sup>1</sup>, L.B. Weinstein<sup>11</sup>, H. Witala<sup>7</sup>

<sup>1</sup>NIKHEF, P.O. Box 41882, 1009 DB Amsterdam, The Netherlands

<sup>2</sup>Universiteit Utrecht, P.O. Box 80.000, 3508 TA Utrecht, The Netherlands

<sup>3</sup>Vrije Universiteit, de Boelelaan 1081, 1081 HV Amsterdam, The Netherlands

<sup>4</sup>Istituto Superiore di Sanità, Laboratorio di Fisica, INFN, Viale Regina Elena 299, Rome, Italy

<sup>5</sup>INFN Sezione di Bari, Dipartimento Interateneo di Fisica, Via Amendola 173, Bari, Italy

<sup>6</sup>Institut für Theoretische Physik II, Ruhr-Universität Bochum, D-44780 Bochum, Germany

<sup>7</sup>Institute of Physics, Jagellonian University, PL-30059 Cracow, Poland

<sup>8</sup>Department of Physics and Astronomy, University of Glasgow, Glasgow G12 8QQ, UK

<sup>9</sup>Department of Physics, University of Regina, Regina SK S4S 0A2, Canada

<sup>10</sup>INFN Sezione di Lecce, via per Arnesano, 73100 Lecce, Italy

<sup>11</sup>Physics Department, Old Dominion University, Norfolk, Virginia 23529

(April 27, 2018)

Cross sections for the  ${}^3\text{He}(e, e'pp)n$  reaction were measured at an energy transfer of 220 MeV and three-momentum transfers  $q$  of 305, 375, and 445 MeV/ $c$ . Results are presented as a function of  $q$  and the final-state neutron momentum for slices in specific kinematic variables. At low neutron momenta, comparison of the data to results of continuum Faddeev calculations performed with the Bonn-B nucleon-nucleon potential indicates a dominant role for two-proton knockout induced by a one-body hadronic current.

PACS numbers: 25.10.+s, 25.30.Fj, 21.45.+v, 21.30.Fe

The ground-state properties of few-nucleon systems are an excellent testing ground for models of the nucleon-nucleon ( $NN$ ) interaction. Calculations of the structure of few-nucleon systems have successfully been performed with realistic  $NN$  potentials, both phenomenological ones and those based on the exchange of mesons and including a phenomenological description of the short-range  $NN$  behaviour [1,2]. The parameters of these models were fitted to the phase shifts obtained from  $NN$  scattering data. Significant advances in solving the three-nucleon ( ${}^3N$ ) continuum [3] currently allow exact calculations of electron-induced nuclear reactions leading to the breakup of the tri-nucleon system [4,5]. The exclusive  ${}^3\text{He}(e, e'NN)N$  reaction is sensitive to details of the initial nuclear state, as well as to the reaction mechanism and rescattering effects in the final state. The three-fold coincidence experiments necessary to measure the cross sections for these reactions have recently proven feasible [6,7].

At intermediate electron energies, the cross section for electron-induced two-nucleon knockout is driven by several processes. The  $NN$  interaction induces initial-state correlations between nucleons and therefore the coupling of a virtual photon to one of these nucleons via a one-body hadronic current can lead to knockout of both nucleons. The interaction of the virtual photon with two-body currents, either via coupling to mesons or via intermediate  $\Delta$  excitation, will also contribute to the cross section. In addition, final-state interactions (FSI)

among the nucleons after absorption of the virtual photon may cause breakup of the tri-nucleon system. By studying the dependence of the cross section on various kinematic quantities one may hope to unravel the tightly connected properties of the  $NN$  interaction, short-range correlations, two-body currents and FSI. In this Letter we present results of a  ${}^3\text{He}(e, e'pp)n$  experiment that was performed in the dip region, i.e., the kinematic domain in between the peaks due to quasi-elastic scattering and  $\Delta$  excitation.

The measurements were performed with the high duty-factor electron beam extracted from the Amsterdam Pulse Stretcher ring at NIKHEF. The incident electrons had an energy of 564 MeV. A cryogenic, high-pressure barrel cell containing gaseous  ${}^3\text{He}$  was used. The luminosity amounted to  $5 \times 10^{35}$  atoms  $\text{cm}^{-2}\text{s}^{-1}$ . The scattered electrons were detected in the QDQ magnetic spectrometer [8] and the emitted protons in highly segmented plastic scintillator arrays [9]. The kinematic settings of the QDQ correspond to a virtual-photon energy of  $\omega=220$  MeV and three-momentum transfer values of  $q=305, 375,$  and  $445$  MeV/ $c$ . At  $q=305$  MeV/ $c$ , protons were detected in the angular ranges  $5^\circ < \gamma_1 < 60^\circ$  and  $-170^\circ < \gamma_2 < -110^\circ$ , where  $\gamma_i$  is the angle between the momentum  $\mathbf{p}'_i$  of proton  $i$  and the transferred three-momentum  $\mathbf{q}$ . For  $q=375$  and  $445$  MeV/ $c$ ,  $\gamma_1$  ranges between  $5^\circ$  and  $30^\circ$ . The acceptance of the second scintillator array is  $\pm 20^\circ$  both in-plane and out-of-plane. The central value of  $\gamma_2$  was chosen such that each configura-

tion includes the point for which the neutron is left at rest. The detection threshold of the proton detectors was 72 and 48 MeV for the kinetic energy of the protons emitted in forward and backward direction, respectively.

Accidental coincidences were subtracted from the measured yield via a procedure described in Ref. [10]. The data were corrected for electronics dead time and for inefficiencies due to multiple scattering and inelastic processes of the protons in the detection systems. Cross sections were obtained by normalizing the yield to the detection volume and integrated luminosity. The results are presented as a function of the missing momentum  $|\mathbf{p}_m| = |\mathbf{q} - \mathbf{p}'_1 - \mathbf{p}'_2|$ , of  $\gamma_1$  and of  $p_{13}$ , defined as  $p_{13} = |\mathbf{p}'_1 - \mathbf{p}'_3|$ .

At missing energies  $E_m = \omega - T_{p'_1} - T_{p'_2} - T_{p'_3}$  below the pion production threshold the kinematics of the  ${}^3\text{He}(e, e'pp)n$  reaction is completely determined, as  $\mathbf{p}'_3 \equiv \mathbf{p}_m$ . The measured missing-energy spectrum contains a peak, corresponding to the three-body breakup of  ${}^3\text{He}$ , which has a width of 6 MeV (FWHM) due to resolutions of the detectors. Strength has been shifted from this peak towards higher missing energies due to radiative processes. The nine-fold differential cross section was integrated over a range in excitation energy up to 14 MeV, taking into account the Jacobian  $\partial T_{p'_2}/\partial E_m$ . The strength beyond this cutoff was estimated with a formalism similar to that for the  $(e, e')$  reaction [11] and applied as an overall correction factor to the data.

In all figures only the statistical errors are indicated. The systematic error on the cross sections is 7%. It is mainly determined by the uncertainty in the integrated luminosity (3%), the uncertainty in the correction applied for hadronic interactions and multiple scattering in the proton detectors (6%), and the determination of the electronics dead time (2%).

The data are compared to results of Faddeev calculations [4], where both the three-nucleon bound-state and final-state wave functions are exact solutions of the  $3N$  Faddeev equations solved in a partial-wave decomposition using the Bonn-B  $NN$  interaction. By including the rescattering contributions to all orders in the continuum, final state interaction effects are taken into account completely. To ensure convergence of the calculations,  $NN$  force components are included up to two-body angular momenta  $j = 3$ .

Two types of calculations were performed. The first one only employs a one-body hadronic current operator. The other one also includes processes, in which the virtual photon interacts with a  $\pi$  or  $\rho$  meson (MECs), either in-flight or in a nucleon-meson vertex. Hence, the hadronic current operator is augmented with additional currents  $\mathbf{j}_\pi$  and  $\mathbf{j}_\rho$  as proposed by Schiavilla *et al.* [12]. At the vertices, cutoff parameters  $\Lambda_\pi = 1.7$  GeV and  $\Lambda_\rho = 1.85$  GeV have been introduced for the  $\pi$  and  $\rho$  meson-exchange interactions to take the finite size of baryons and mesons into account. In the case of direct

two-proton knockout, the contribution of MECs to the cross section is suppressed, as the virtual photon – to first relativistic order – cannot interact with a neutral meson exchanged in a  $pp$  system.

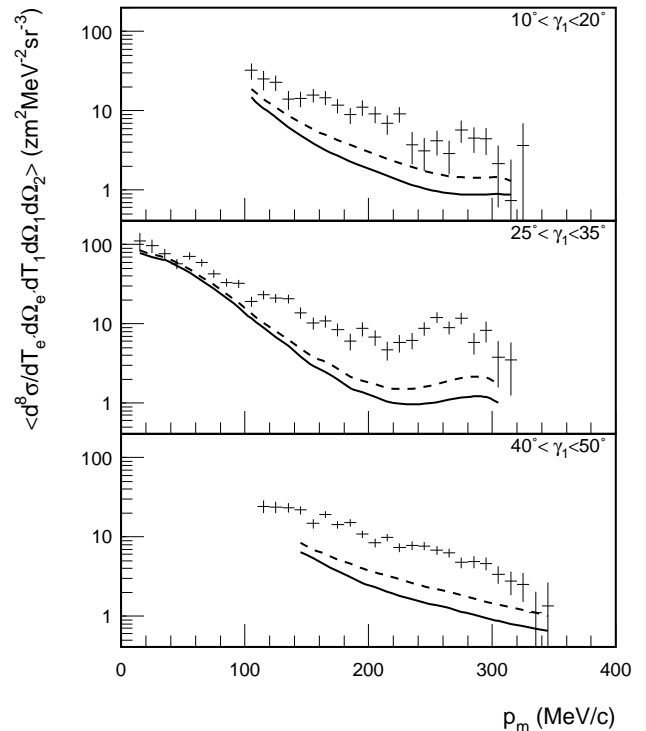


FIG. 1. The averaged eight-fold differential cross section for the reaction  ${}^3\text{He}(e, e'pp)$  for the kinematic setting  $(\omega, q) = (220 \text{ MeV}, 305 \text{ MeV}/c)$  as a function of the missing momentum. The data were averaged over the  $\gamma_2$  range from  $114^\circ$  to  $142^\circ$  for three slices of  $\gamma_1$ . The solid (dashed) curves represent the results of continuum Faddeev calculations without (including) MECs.

The calculation of the differential cross section was performed in two stages. The process of solving the Faddeev equations, which is computationally the most involved, was performed once per given  $(\omega, q)$  setting. Cross sections could subsequently be calculated for specific three-nucleon final states, determined by  $\mathbf{p}'_1$  and  $\mathbf{p}'_2$ . This is especially important when comparing theoretical predictions to data obtained with large-acceptance detectors, since the cross section varies significantly within the region of phase space covered by the experimental detection volume. An orthogonal grid in the laboratory quantities  $(\theta_1, \phi_1, \theta_2, \phi_2, T_1)$  was employed to compute the cross section in each bin by averaging over the contributing part of the experimental phase space. A sufficiently large number of grid points ( $2.5 \times 10^6$  points per setting) was taken to ensure convergence within 5%.

The cross sections measured at  $q = 305 \text{ MeV}/c$  are shown in Fig. 1 as a function of the neutron momentum ( $p'_3 \equiv p_m$ ) in the final state. The three panels corre-

spond to different ranges in  $\gamma_1$ . The largest range in  $p_m$  is spanned for  $25^\circ < \gamma_1 < 35^\circ$ . Here, the cross section was determined down to  $p_m$  values as low as 10 MeV/c. In all panels the cross sections decrease roughly exponentially with approximately the same slope as a function of  $p_m$ . This decrease reflects the neutron momentum distribution inside  ${}^3\text{He}$ , for a specific range of  $pp$  relative momenta. In the measured configuration the domain of relative momenta around 300 MeV/c per nucleon was probed. The curves show the results of continuum Faddeev calculations. The solid curve represents results obtained with a one-body hadronic current only, while the dashed line also includes contributions due to MECs. As can be seen in the middle panel, for  $p_m \lesssim 100$  MeV/c there is a fair description of the data by the solid curve and the contribution due to MECs is almost negligible.

At higher missing momenta calculations including only one-body currents fall short by about a factor of five. The discrepancy between data and calculations is likely to be due to two-body hadronic processes, which involve coupling of the virtual photon to a proton-neutron system in the initial state, thus generating neutrons with a large momentum in the final state. This is reflected in the increase of the MEC contribution from 5% to 40% of the calculated cross section towards high  $p_m$ , which is clearly not enough to explain the discrepancy with the data.

Also excitation of the  $\Delta$  resonance followed by its nonmesonic decay has to be considered. The contribution of this process strongly depends on the invariant mass  $W_{\gamma NN}$  of the virtual photon plus two-nucleon system. In a direct reaction mechanism, i.e., at low  $p_m$ , this is equal to the invariant mass of the two-proton system in the final state,  $W_{p'_1 p'_2}$ . For all kinematic settings we have  $2030 \lesssim W_{p'_1 p'_2} \lesssim 2055$  MeV/c<sup>2</sup>, which is well below the mass of the  $N\Delta$  system. Moreover, in the two-proton case the contribution of  $pp \rightarrow \Delta^+ p \rightarrow pp$  will be further suppressed because of angular-momentum and parity conservation selection rules. At high  $p_m$  intermediate  $\Delta$  excitation via the absorption of the virtual photon by a  $pn$  pair will contribute substantially to the reaction. This process is known to dominate the  $(\gamma, pn)$  reaction at  $E_\gamma > 180$  MeV [13]. The invariant mass  $W_{p' n'}$  of a  $pn$  system at  $p_m \approx 300$  MeV/c is around 2130 MeV/c<sup>2</sup>, which is close to the resonant mass of the  $N\Delta$  system.

It should be noted that – for a fixed value of  $p_m$  – the angle  $\gamma_1$  implicitly defines the kinematic configuration of the final state, provided that the direction of  $\mathbf{p}'_2$  is kept within a limited range. For  $\gamma_1 \lesssim 25^\circ$  and  $\gamma_1 \gtrsim 35^\circ$ , the three nucleons are always emitted at sizeable angles with respect to each other, which reduces their mutual interactions. Enhanced probability for rescattering occurs in so-called ‘FSI configurations’ where two nucleons are emitted with approximately the same momentum and angle. Within the interval  $25^\circ < \gamma_1 < 35^\circ$ , an ‘FSI configuration’ between proton-1 and the undetected neutron

occurs around  $p_m = 300$  MeV/c, which introduces the bump observed in the data for  $200 \lesssim p_m \lesssim 300$  MeV/c. A similar structure is seen in the calculated curves.

The enhanced rescattering effects occurring around ‘FSI configurations’ are the dominant factor that determines the cross section in these regions. The occurrence of such configurations can not be avoided in experiments with large-solid-angle detectors. On the other hand, their presence offers the possibility to test the treatment of FSI in calculations. For these kinematic conditions, the cross section is best represented as a function of the momentum difference between the two outgoing nucleons involved:  $p_{ij} = |\mathbf{p}'_i - \mathbf{p}'_j|$ . Here  $p_{ij} = 0$  MeV/c corresponds to the actual ‘FSI configuration’.

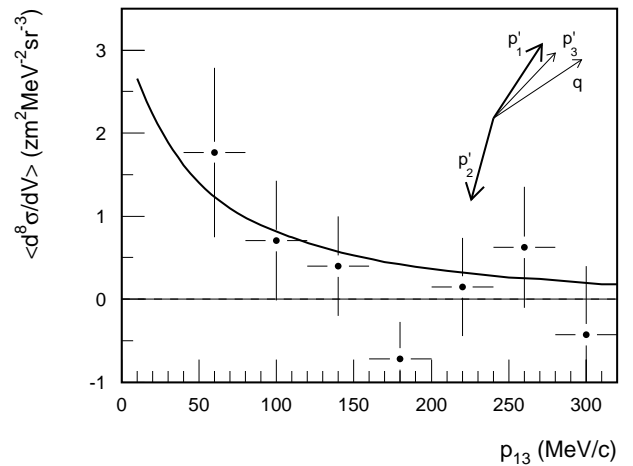


FIG. 2. Average cross section as a function of the momentum difference  $p_{13}$  for the proton-neutron ‘FSI configuration’ in the  $(\omega, q) = (220 \text{ MeV}, 445 \text{ MeV}/c)$  kinematic setting. The solid curve represents the continuum Faddeev result obtained with a one-body hadronic current. A schematic representation of the kinematics is indicated.

As mentioned before, the influence of such an ‘FSI configuration’ is already apparent in Fig. 1 at  $p_m \approx 250$  MeV/c and  $\gamma_1 \approx 30^\circ$ . Figure 2 shows the cross section as a function of  $p_{13}$  for the measurements at  $q=445$  MeV/c, where the detection volume extends to  $p_{13} = 0$  MeV/c. The acceptance in  $p_m$  has been limited to  $380 < p_m < 400$  MeV/c to ensure complete coverage of the detection volume for the entire domain  $0 < p_{13} < 320$  MeV/c. This also limits  $p'_1$  to the range 380–430 MeV/c. The range in  $p_{13}$  is therefore mainly due to angular variations between the undetected neutron and the forward proton. A typical final-state configuration is shown in the inset of Fig. 2.

The cross section data presented in Fig. 2 show an increase as  $p_{13}$  approaches 0 MeV/c. This trend is well reproduced by the continuum Faddeev calculations which include rescattering among the three outgoing nucleons.

Figure 3 shows the dependence of the cross section on the three-momentum transfer  $q$ . As the cross section is

primarily determined by the momentum of the neutron, the data are presented for two regions in  $p_m$ . The region above  $p_m=220$  MeV/c is disregarded in this discussion as ‘FSI configurations’ occur in this domain and the cross section is affected differently at various values of  $q$ .

For  $20 < p_m < 120$  MeV/c the reaction can be considered as a direct process, leaving the spectator neutron ‘at rest’ in the final state. The measured cross section decreases by a factor of four between  $q=305$  and  $375$  MeV/c. The agreement in size and slope between the data and the continuum Faddeev calculations performed with a one-body hadronic current, suggests that in this domain the cross section is dominated by knockout of correlated proton pairs. For  $120 < p_m < 220$  MeV/c theory underestimates the data for all three  $q$  values by a factor of five.

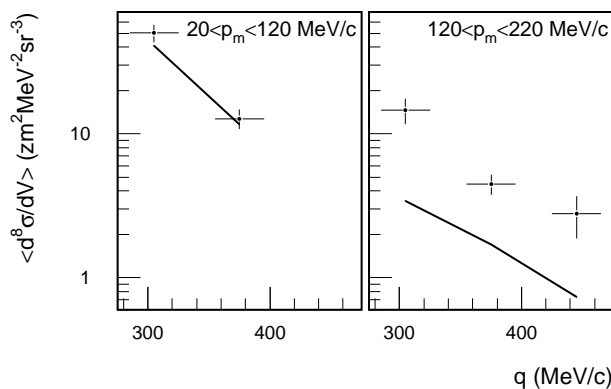


FIG. 3. Averaged cross section for three values of the virtual-photon momentum at an energy transfer of 220 MeV. The cross sections were averaged over  $10^\circ < \gamma_1 < 25^\circ$  and the indicated missing-momentum intervals. The horizontal error bars indicate the range covered in  $q$  by the acceptance of the spectrometer. The curves represent the results of continuum Faddeev calculations with a one-body hadronic current.

In conclusion, differential cross sections for the  ${}^3\text{He}(e, e'pp)$  reaction were measured at  $\omega=220$  MeV and  $q=305, 375,$  and  $445$  MeV/c with good statistical accuracy. The measured cross section decreases roughly exponentially as a function of  $p_m$  in the domain from 10 to 350 MeV/c. Continuum Faddeev calculations using the Bonn-B  $NN$  potential, which include rescattering of the outgoing nucleons to all orders and also take meson-exchange currents into account, describe the data reasonably well for  $p_m < 100$  MeV/c. However, an increasing discrepancy up to a factor three is observed at larger  $p_m$  values. In this domain meson-exchange currents account for 40% of the calculated cross section and also intermediate  $\Delta$  excitation, especially in the  $pn$  system, is expected to contribute strongly to the cross section in this domain. Comprehensive treatment of intermediate  $\Delta$  excitation in the calculations is needed for a detailed interpretation of the data in this high  $p_m$  region. Rescattering of the nu-

cleons in the final state influences the cross section in specific kinematic orientations; within such a subset of the data, the observed trend is well reproduced by the results of the continuum Faddeev calculations.

At small  $p_m$  values the dependence of the cross section on  $q$  is indicative for direct knockout of two protons by a virtual photon. The fair agreement between the data and calculations based on a one-body hadronic current indicates that in this domain the cross section mainly originates from knockout of two correlated protons. This opens the opportunity to exploit this low  $p_m$  domain for a detailed study of  $pp$  correlations in few-nucleon systems.

This work is part of the research program of the Foundation for Fundamental Research on Matter (FOM) and was sponsored by the Stichting Nationale Computerfaciliteiten (National Computing Facilities Foundation, NCF) for the use of supercomputer facilities. Both organisations are financially supported by the Netherlands Organisation for Scientific Research (NWO). The support of the Science and Technology Cooperation Germany-Poland, the Polish Committee for Scientific Research (grant No. 2P03B03914), and the US Department of Energy is gratefully acknowledged. Part of the calculations have been performed on the Cray T90 and T3E of the John von Neumann Institute for Computing, Jülich, Germany.

\* Electronic correspondence may be addressed to eddy@nikhef.nl.

- [1] A. Nogga, D. Hüber, H. Kamada, W. Glöckle, Phys. Lett. B **409**, 19 (1997).
- [2] J. Carlson, R. Schiavilla, Rev. Mod. Phys. **70**, 743 (1998).
- [3] W. Glöckle *et al.*, Phys. Rep. **274**, 107 (1996).
- [4] J. Golak *et al.*, Phys. Rev. C **51**, 1638 (1995).
- [5] E. van Meijgaard, J.A. Tjon, Phys. Rev. C **45**, 1463 (1992).
- [6] C.J.G. Onderwater *et al.*, Phys. Rev. Lett. **78**, 4893 (1997).
- [7] G. Rosner, in *Proceedings of the Conference on Perspectives in Hadronic Physics*, ed. S. Boffi, C. Ciofi degli Atti, and M.M. Giannini (ICTP, World Scientific, Singapore, 1997), p. 185.
- [8] C. de Vries *et al.*, Nucl. Instrum. Methods Phys. Res., **223**, 1 (1984).
- [9] A.R. Pellegrino *et al.*, accepted for publication in Nucl. Instrum. Methods Phys. Res., Sect. A.
- [10] C.J.G. Onderwater *et al.*, Phys. Rev. Lett. **81**, 2213 (1998).
- [11] L.W. Mo, Y.S. Tsai, Rev. Mod. Phys. **41**, 205 (1969).
- [12] R. Schiavilla, V.R. Pandharipande, D.O. Riska, Phys. Rev. C **40**, 2294 (1989).
- [13] S. Boffi, C. Giusti, F.D. Pacati, M. Radici, Nucl. Phys. **A564**, 473 (1993).